Contribution from the Department of Chemistry,
McMaster University, Hamilton, Ontario, L8S 4M1, Canada

The KrF^+ and $Kr_2F_3^+$ Cations. The Preparation of $KrF^+MF_6^-$, $KrF^+Sb_2F_{11}^-$, $Kr_2F_3^+MF_6^-$, and $Kr_2F_3^+ \cdot xKrF_2 \cdot MF_6^-$ Salts and Their Characterization by Fluorine-19 Nuclear Magnetic Resonance and Raman Spectroscopy[1]

R. J. GILLESPIE* and G. J. SCHROBILGEN

Received January 14, 1975 AIC50032P

The reactions of KrF_2 with AsF_5, SbF_5, and PtF_6 have been studied by ^{19}F nuclear magnetic resonance spectroscopy and Raman spectroscopy. The following compounds have been prepared and characterized: $KrF^+AsF_6^-$ (low- and high-temperature forms), $KrF^+SbF_6^-$, $KrF^+PtF_6^-$, $KrF^+Sb_2F_{11}^-$, $Kr_2F_3^+AsF_6^-$, and $Kr_2F_3^+SbF_6^-$. The ^{19}F NMR spectrum shows that in solution in BrF_5 $Kr_2F_3^+$ has a symmetrical fluorine-bridged structure like that of $Xe_2F_3^+$. Although the Raman spectrum is reasonably consistent with such a structure it can also be interpreted as indicating that the cation has an unsymmetrical structure in the solid state. $Kr_2F_3^+$ reacts further with KrF_2 to give another species $Kr_2F_3^+ \cdot xKrF_2$ whose exact composition and nature are still uncertain.

Introduction

Until recently, the only well-characterized compounds of krypton were the difluoride[2,3] and the adduct $KrF_2 \cdot 2SbF_5$.[4] It had also been reported that KrF_2 forms a solid adduct with AsF_5 at −78°, but this solid was not characterized.[4] More recently, Bartlett et al.[5] have repeated the preparation of the antimony pentafluoride complex and have obtained the Raman spectrum. On the basis of the known structure of the corresponding $XeF_2 \cdot 2SbF_5$[6] compound and the similarity of the Raman spectra of $XeF_2 \cdot 2SbF_5$[7,8] and $KrF_2 \cdot 2SbF_5$, the latter compound has been formulated as the salt $KrF^+Sb_2F_{11}^-$. Subsequent to the completion of our work, Frlec and Holloway[9] also reported the preparation and Raman spectra of $KrF_2 \cdot 2TaF_5$, $KrF_2 \cdot TaF_5$, and $KrF_2 \cdot 2NbF_5$ and they have obtained limited Raman spectral evidence for the existence of the $Kr_2F_3^+$ cation in the solid phase.

In the present work two salts of the $Kr_2F_3^+$ cation have been prepared and unambiguously characterized by ^{19}F NMR and Raman spectroscopy. A new type of adduct which is formulated as $Kr_2F_3^+ \cdot xKrF_2 \cdot MF_6^-$ and which may be $Kr_3F_5^+ \cdot MF_6^-$ has also been prepared. In addition, the ^{19}F NMR and Raman spectra of several KrF^+ salts have been obtained. Some of this work has been briefly described in a preliminary communication.[10] In a simultaneous preliminary publication[11] Holloway and Frlec described the preparation and characterization of $KrF^+SbF_6^-$ and $Kr_2F_3^+SbF_6^-$ by Raman spectroscopy. Further details of their work appear in a forthcoming paper.[12] We have described elsewhere the use of KrF^+ and $Kr_2F_3^+$ as oxidative fluorinating agents for the preparation of BrF_6^+ from BrF_5.[10,13]

Results and Discussion

Syntheses, Properties, and Reactions. The SbF_5 and AsF_5 adducts were formed by the series of reactions given in Schemes I and II, respectively. The progress of each reaction was monitored by Raman spectroscopy by periodically quenching the reaction at −196° and recording the Raman spectrum at −90°. The Raman spectra of the products, as discussed below, are consistent with the ionic formulations given in these schemes.

Both $KrF^+Sb_2F_{11}^-$ and $KrF^+SbF_6^-$ are stable white solids at room temperature. The reaction of $KrF^+Sb_2F_{11}^-$ with an additional mole of KrF_2 at 25° to give $KrF^+SbF_6^-$ is slowly reversible under dynamic vacuum at room temperature. Addition of a large excess of KrF_2 to $KrF^+SbF_6^-$ results in a pale yellow-green mixture at 0° which fuses at 25° and rapidly decomposes exothermically to Kr, F_2, and $KrF^+SbF_6^-$. Judicious cooling and warming of the mixture results in a slow, smooth decomposition of excess KrF_2 to give a pale yellow-green compound at room temperature which has a solid

Scheme I

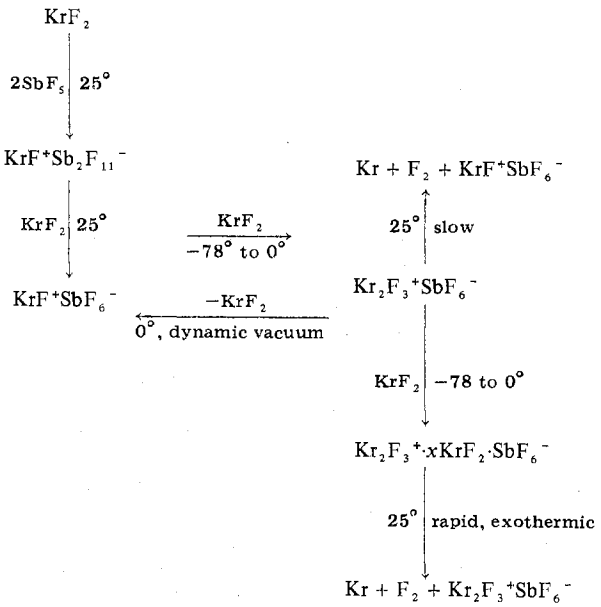

Scheme II

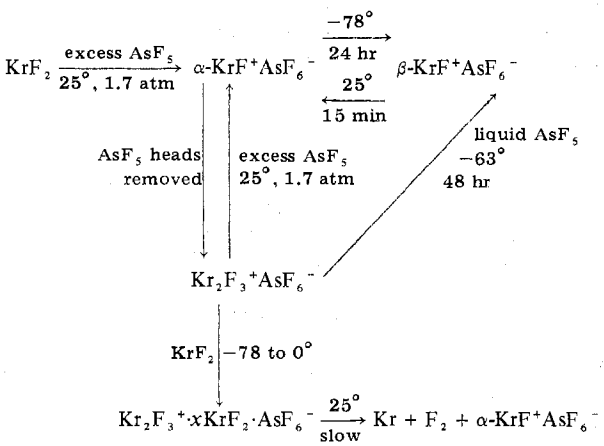

state Raman spectrum and a low-temperature ^{19}F NMR spectrum (in BrF_5 solvent) which corresponds to $Kr_2F_3^+SbF_6^-$. The $Kr_2F_3^+$ salt rapidly decomposes under vacuum at 0° to give $KrF^+SbF_6^-$ and also undergoes a slow decomposition to Kr, F_2, and $KrF^+SbF_6^-$ at room temperature under 1.7 atm of argon gas. Addition of a large excess of KrF_2 to either $Kr_2F_3^+SbF_6^-$ or $KrF^+SbF_6^-$ gives another adduct which is stable at low temperatures, but very unstable at room tem-

Table I. ^{19}F NMR Parameters for $Kr_2F_3^+$, KrF^+, KrF_2, and Their Xenon Analogues

Solutes (*m* concn)	Solvent	Temp, °C	J_{FF}, Hz BrF_5	J_{FF}, Hz $Ng_2F_3^+$	Chemical shift, ppm[a,b] $Ng_2F_3^+$	NgF^+	NgF_2	Anion	Solvent
(1) KrF_2 (0.22)	HF	26					−55.6		199.2
(2) KrF_2 (0.80)	BrF_5	27	75				−77.7		A −275.9; X_4 −139.0
		−50	75				−67.9		A −272.6; X_4 −135.5
(3) KrF_2 (0.22) SbF_5 (4.96)	HF	−40				22.6		92[c], 119[c], 139[c], 124[c] $Sb_2F_{11}^-$, SbF_6^-	192.4
(4) $Kr_2F_3^+SbF_6^-$ (~0.5)	BrF_5	−65		347	A −18.8; X_2 −73.4			115	−156[d]
(5) $Kr_2F_3^+AsF_6^-$ (~0.5)	BrF_5	−65		347	A −19.0; X_2 −73.8			*e*	−150[e]
(6) KrF_2 (~1.5)[f] SbF_5 (~0.5)[f]	BrF_5	−65	75	351	A −19.2; X_2 −73.6		−65.5	120	A −276.4; X_4 −136.8
(7) KrF_2 (~1.0)[g] SbF_5 (~0.5)[g]	BrF_5	−66	75	351	A −19.0; X_2 −73.6			123	A −276.9; X_4 −137.0
(8) XeF_2 (sat soln)	HF	−68					199.6 (5665)		−195.4
(9) XeF_2 (1.85)	BrF_5	26	75				181.8 (5645)		A −272.9; X_4 −138.1
		−20	75				181.8 (5650)		A −271.3; X_4 −136.2
(10) XeF_2 (0.34)	SbF_5	26				289.8 (7210)		*h*	111.1[h]
(11) $Xe_2F_3^+AsF_6^-$ (0.67)	BrF_5	−62	75	308	A 184.7 (4865); X_2 252.0 (6740)			61.8	A −272.8; X_4 −134.3

[a] With respect to external $CFCl_3$. [b] Values in parentheses represent the ^{129}Xe-^{19}F coupling constant (Hz). [c] The spectrum is similar to that previously observed for high concentrations of SbF_5 dissolved in HF: R. J. Gillespie and K. C. Moss, *J. Chem. Soc. A*, 1170 (1966). [d] Axial and equatorial fluorine environments of BrF_5 collapsed into a single broad exchange-averaged peak. [e] The peak represents AsF_6^- and the fluorine environments of BrF_5 undergoing rapid fluorine exchange. [f] KrF_2:SbF_5 calculated from the integrated KrF_2 and $Kr_2F_3^+$ peaks was 3:3:1. [g] Solution 6 after warming to room temperature for several seconds. [h] $SbF_5/Sb_nF_{5n+1}^-$ undergoing rapid fluorine exchange.

perature, and which we formulate as $Kr_2F_3^+ \cdot xKrF_2 \cdot SbF_6^-$ and which may be $Kr_3F_5^+SbF_6^-$.

The KrF_2–AsF_5 system is more complex. Reaction of KrF_2 with AsF_5 at room temperature leads directly to the high-temperature phase, α-$KrF^+AsF_6^-$. This compound is unstable at room temperature and slowly decomposes, liberating Kr, F_2, and AsF_5. Cooling to −78° results in a slow transition giving the low-temperature phase, β-$KrF^+AsF_6^-$. The reverse process occurs rapidly upon warming to room temperature. Removal of volatile heads from α-$KrF^+AsF_6^-$ results in a new salt which is formulated as $Kr_2F_3^+AsF_6^-$. Analogous behavior is exhibited by $XeF^+AsF_6^-$ which slowly decomposes according to eq 1 under dynamic vacuum at room temperature.[7,14]

$$2XeF^+AsF_6^- \xrightarrow{\text{vacuum}} Xe_2F_3^+AsF_6^- + AsF_5 \quad (1)$$

Reaction of $Kr_2F_3^+AsF_6^-$ with excess AsF_5 occurs rapidly at room temperature to give α-$KrF^+AsF_6^-$ and slowly at −63° to give β-$KrF^+AsF_6^-$. Like the analogous SbF_6^- compounds, α-$KrF^+AsF_6^-$ and $Kr_2F_3^+AsF_6^-$ were found to react with excess KrF_2 to give the corresponding $Kr_2F_3^+ \cdot xKrF_2AsF_6^-$ compound.

The reactions of PtF_6 with oxygen,[15] xenon,[16] and nitric oxide[17] have established its remarkable oxidizing power. Although few reactions are known which spontaneously liberate molecular fluorine at low temperature, such reactions are a relatively common feature of the chemistry of PtF_6 and IrF_6,[17] e.g.,

$$FNO + PtF_6 \rightarrow NO^+PtF_6^- + {}^1/_2F_2 \quad (2)$$

The related reaction of PtF_6 with KrF_2 according to eq 3,

$$KrF_2 + PtF_6 \rightarrow KrF^+PtF_6^- + {}^1/_2F_2 \quad (3)$$

which gives a canary-yellow solid, formulated as $KrF^+PtF_6^-$, and molecular fluorine, is consistent with the apparently very high electron affinity of PtF_6. Although $KrF^+SbF_6^-$, $KrF^+Sb_2F_{11}^-$, and $KrF^+PtF_6^-$ are all stable in the solid phase at room temperature, solutions of $KrF^+SbF_6^-$ and $KrF^+PtF_6^-$ in anhydrous HF, KrF_2 in SbF_5, and $Kr_2F_3^+MF_6^-$ and $KrF^+MF_6^-$ (M = As or Sb) in BrF_5 are all unstable and decompose rapidly at room temperature according to eq 4 and 5. In the case of the BrF_5 solvent, some of the BrF_5 is also

$$Kr_2F_3^+MF_6^- \rightarrow KrF^+MF_6^- + Kr + F_2 \quad (4)$$

$$KrF^+MF_6^- \rightarrow MF_5 + Kr + {}^1/_2F_2 \quad (5)$$

oxidized to the previously unknown BrF_6^+ cation at room temperature.[10,13] In contrast, solutions of KrF_2 in BrF_5 or HF are stable for up to several hours at room temperature. It would appear that the KrF^+ and $Kr_2F_3^+$ ions are markedly less stable in solution than in the solid state and are also less stable than KrF_2 in solution.

The salts of KrF^+ are extremely powerful oxidants and rapidly oxidize gaseous O_2 and Xe to O_2^+ and XeF^+, respectively, at room temperature. The reactions were carried out in the presence of 1.7 atm of O_2 or Xe gas and proceed according to eq 6 and 7. In both cases, lines attributed to

$$O_2 + \alpha\text{-}KrF^+AsF_6^- \rightarrow O_2^+AsF_6^- + Kr + {}^1/_2F_2 \quad (6)$$

$$Xe + \alpha\text{-}KrF^+AsF_6^- \rightarrow XeF^+AsF_6^- + Kr \quad (7)$$

α-$KrF^+AsF_6^-$ in the low-temperature Raman spectrum disappeared, the AsF_6^- lines being replaced by a new set of AsF_6^- lines slightly shifted in frequency. In addition, single intense bands appeared at 1857 cm^{-1} (reaction with O_2) and 609 cm^{-1} (reaction with Xe) which can only be assigned to the O_2^+ [18] and XeF^+ [8] stretching vibrations, respectively.

^{19}F NMR Spectroscopy. A solution of KrF_2 in HF gave a single resonance at −55.6 ppm, in good agreement with the previously reported value of −53 ppm.[2] Transfer of the solution to a sample tube containing an excess of SbF_5 with respect to KrF_2 gave a new signal to high field of KrF_2 (Table I). This new signal can be assigned to KrF^+ and the high-field

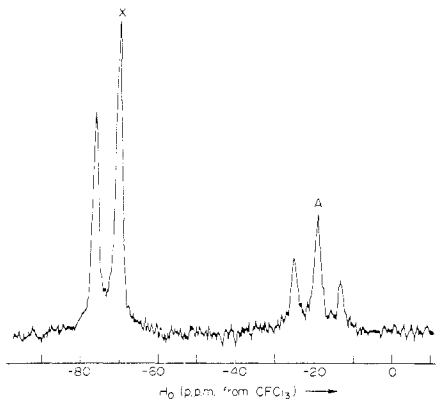

Figure 1. The ^{19}F NMR spectrum (58.3 MHz, −66°) of the $Kr_2F_3^+$ cation (~0.5 *m* $Kr_2F_3^+SbF_6^-$ in BrF_5 solvent): (A) bridging fluorine; (X) terminal fluorines.

shift is analogous to that observed when XeF_2 ionizes to give XeF^+ (Table I).

In the case of both KrF^+ and XeF^+ the chemical shift from the parent KrF_2 and XeF_2 molecules is in the opposite direction to that of the Xe(IV) and Xe(VI) fluoro- and oxyfluorocations which all have chemical shifts to low field of the parent molecule.[19-21]

Bromine pentafluoride solutions of $Kr_2F_3^+AsF_6^-$ and $Kr_2F_3^+SbF_6^-$ as well as solutions containing KrF_2 and SbF_5 in a 2:1 mol ratio gave identical AX_2 spectra at low temperatures (Figure 1 and Table I) which can be unambiguously assigned to the V-shaped fluorine-bridged structure (I) similar to that which has previously been established by x-ray crystallography for $Xe_2F_3^+$.[14] It is noteworthy that the

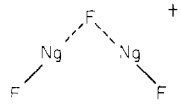

I

terminal resonance of $Kr_2F_3^+$ occurs to low field of the bridging fluorine while the opposite is true in the case of $Xe_2F_3^+$ (Table I). The relatively large fluorine–fluorine coupling constant (349 Hz), which is the first observed for a krypton compound, is, however, similar to the value observed for $Xe_2F_3^+$ (308 Hz). In the other fluoro- and oxyfluorocations of xenon characterized to date, the fluorine–fluorine coupling constant is comparatively small (103–176 Hz).[19-21] It is possible that the large difference between the values of $Xe_2F_3^+$ and $Kr_2F_3^+$ and those for the other cations may be associated with the fact that the F–Ng–F angle is ~180° in $Xe_2F_3^+$ and $Kr_2F_3^+$, but is only ~90° in the other cations.

The chemical shift of krypton difluoride in BrF_5, unlike that of XeF_2, shows a considerable temperature dependence (Table I). The phase diagram of the KrF_2–BrF_5 system[22] indicates that the solvates $KrF_2 \cdot 9BrF_5$, $KrF_2 \cdot 2BrF_5$, and $KrF_2 \cdot BrF_5$ are formed in the system at low temperatures. It therefore seems reasonable to attribute the temperature dependence on the chemical shift to the equilibria

$$KrF_2 + nBrF_5 \rightleftarrows KrF_2 \cdot nBrF_5 \quad (8)$$

The ^{19}F NMR spectrum of a BrF_5 solution containing KrF_2:SbF_5 = 3.3:1 gave no evidence for a further interaction between KrF_2 and $Kr_2F_3^+$ in solution (Table I), as is indicated by the Raman spectra of the solid phase, but consisted of a simple composite of the KrF_2 and $Kr_2F_3^+SbF_6^-$ spectra.

Whereas BrF_5 solutions of KrF_2 in the absence of $Kr_2F_3^+SbF_6^-$ are stable for up to several hours at room temperature, warming a solution of KrF_2 in the presence of $Kr_2F_3^+SbF_6^-$ to ~0° for a few seconds resulted in rapid evolution of krypton and fluorine and a corresponding decrease in the intensity of the KrF_2 line in the ^{19}F NMR spectrum. The decomposition was allowed to proceed until the KrF_2 line had just vanished. At this point separate lines due to BrF_5 and $Kr_2F_3^+$, both with well-resolved fine structures, and SbF_6^- were still visible in the low-temperature spectrum. The integrated relative intensities of the fluorine-on-krypton and fluorine-on-antimony portions of the spectrum were 1:2, respectively, thus confirming the proposed stoichiometry $Kr_2F_3^+SbF_6^-$. Continued warming resulted in a decrease in the intensity of the $Kr_2F_3^+$ lines relative to SbF_6^- and collapse of the fluorine-on-bromine peak into a single exchange-averaged line. The decomposition presumably proceeds according to eq 9 producing KrF^+, which in turn catalyzes an exchange according to eq 10. This exchange is also responsible

$$Kr_2F_3^+ \rightarrow KrF^+ + Kr + F_2 \quad (9)$$

$$KrF^+ + BrF_5 \rightleftarrows KrF_2 + BrF_4^+ \quad (10)$$

for collapse of the BrF_5 solvent peaks in solutions of the pure $Kr_2F_3^+AsF_6^-$ and $Kr_2F_3^+SbF_6^-$ salts (Table I). In both instances a small quantity of KrF^+ was presumably generated when the samples were warmed briefly to ca. −20° to effect dissolution. Unlike the SbF_6^- salt, the AsF_6^- salt did not give a separate peak due to the anion. This is a consequence of additional exchange reactions involving the more strongly basic AsF_6^- anion, and may be due to equilibria 11 and 12.

$$KrF^+ + AsF_6^- \rightleftarrows KrF_2 + AsF_5 \quad (11)$$

$$BrF_5 + AsF_5 \rightleftarrows BrF_4^+ + AsF_6^- \quad (12)$$

Raman Spectroscopy. $KrF^+MF_6^-$ and $KrF^+Sb_2F_{11}^-$. The Raman spectra of these compounds are given in Figure 2 and Tables II and III. The Kr–F stretching frequency in the $Sb_2F_{11}^-$ compound is in excellent agreement with that recently reported by Bartlett and coworkers[5] and by Frlec and Holloway.[9] A recent ab inito calculation on KrF^+ ion predicts a value for ν(Kr–F) of 621 cm^{-1}.[23] The excellent agreement with the experimental value in several KrF^+ compounds, which has also been cited by other workers,[5,9] must, however, be considered in part fortuitous since the calculated frequency is only reliable to about ±60 cm^{-1} and the gas-phase frequency would be expected to differ somewhat from that observed in the solid. Splitting of ν(Kr–F) into a doublet occurs in $KrF^+SbF_6^-$, $KrF^+PtF_6^-$, and in both the high-temperature (α) and the low-temperature (β) phases of $KrF^+AsF_6^-$, and may be attributed to weak intermolecular coupling (factor-group splitting) of the cation modes. On the basis of the size of the splitting, the relative intensities of the doublet lines, and the frequency of the Kr–F stretching modes, two types of salts may be distinguished: one exemplified by $KrF^+SbF_6^-$ and β-$KrF^+AsF_6^-$, which appear to be isomorphous, and another by $KrF^+PtF_6^-$ and α-$KrF^+AsF_6^-$, which also appear to be isomorphous.

The normal modes of a highly symmetric anion such as MF_6^- can serve as a sensitive probe for the detection of significant anion–cation interactions. An isolated MF_6^- ion possesses O_h symmetry and the resulting six normal modes of vibration are classified as $a_{1g} + e_g + 2\,t_{1u} + t_{2g} + t_{2u}$. Of these only the two t_{1u} modes are infrared active, while only the a_{1g}, e_g, and t_{2g} modes are Raman active. The remaining t_{2u} mode is inactive in both the infrared and Raman spectra. Thus only four frequencies, including the Kr–F stretch, are expected in the Raman spectrum of a purely ionic $KrF^+MF_6^-$ in the solid state provided that the site symmetry for MF_6^- is also O_h. A considerably larger number of bands are however observed in the spectra of the $KrF^+MF_6^-$ salts listed in Table II. Although this increased number of bands may, in principle, be attributed simply to a site symmetry lowering because bands have also been observed that may reasonably be assigned to vibrational modes of the F–Kr---F group, we prefer to consider that it is

Table II. Raman Spectra and Assignments for Some $KrF^+MF_6^-$ Salts and Their Xenon Analogues

Frequency, cm^{-1} [a]								
$KrF^+SbF_6^-$	β-$KrF^+AsF_6^-$	α-$KrF^+AsF_6^-$	$KrF^+PtF_6^-$	XeF^+-SbF_6^- [c]	XeF^+-AsF_6^- [c]	XeF^+-PtF_6^- [d]	XeF^+-IrF_6^- [d]	Assignments[b]
619 (74) 615 (100)	619 (72) 615 (100)	607 (100) 596 (100)	606 (50) 599 (60)	615 (100)	609 (100)	609 (23) 602 (35)	608 (44) 602 (60)	$\nu_1(a_1)$, ν(Ng–F)
338 (4)	338 (16)	328 (12)	338 (3)	337 (6)	339 (21)			$\nu_2(a_1)$, ν(Ng- - -F)
169 (5) 162 (7) 145 (3)	173 (10) 162 (11)	173 (8)	169 (3) 139 (8)	141 (23)	155 (15) 146 (sh, 8)			$\nu_3(e)$, δ(F–Ng- - -F)
664 (45)	676 (13)	679 (7)	658 (100)	666 (43)	678 (20)	655 (100)	679 (100)	$\nu_1(a_1)$, (F- - -MF_5)$^-$
642 (10)	595 (5)		587 (6)	645 (15)	667 (4)	592 (18)	564 (13)	$\nu_2(a_1)$, (F- - -MF_5)$^-$
586 (5)			581 (6)	586 (6)	586 (10)	580 (14)		$\nu_5(b_1)$, (F- - -MF_5)$^-$
480 (4) 462 (8)	464 (3)	453 (1)	519 (2) 504 (12)	467 (15) 447 (13)	443 (3)		498 (~10)	$\nu_4(a_1)$, (F- - -MF_5)$^-$
682 (3)	716 (16)	713 (8)	630 (38)	685 (6)	731 (5) 724 (5)	637 (28) 627 (46)	633 (20)	$\nu_8(e)$, (F- - -MF_5)$^-$
266 (6)	419 (sh) 411 (10)	417 (9)	266 (1)	267 (11)	417 (5)			$\nu_3(a_1)$, (F- - -MF_5)$^-$
255 (6) 214 (2)	273 (1)	276 (1)	229 (11) 222 (10)			230 (24)	230 (20)	$\nu_{11}(e)$, (F- - -MF_5)$^-$
	366 (9)	371 (1)	350 (3)	388 (4)				$\nu_7(b_2)$, (F- - -MF_5)$^-$
288 (9)	384 (4)	383 (5)	248 (2)	290 (11)	387 (6)	246 (17)	256 (30)	$\nu_9(e)$, (F- - -MF_5)$^-$
				180 (4)	180 (2)			$\nu_6(b_1)$, (F- - -MF_5)$^-$
	395 (1)							$\nu_{10}(e)$, (F- - -MF_5)$^-$

[a] The Raman spectra of all of the KrF^+ salts, with the exception of $KrF^+PtF_6^-$, were recorded at −90° in FEP sample tubes using the 5145 Å exciting line. Lines due to the FEP sample tube have been deleted. [b] Approximate descriptions of the MF_6^- modes under C_{4v} symmetry are given in Table IV. [c] Reference 8. [d] Reference 7.

Table III. Raman Spectra of $KrF^+Sb_2F_{11}^-$ and $XeF^+Sb_2F_{11}^-$

Frequency, cm^{-1}		
$KrF^+Sb_2F_{11}^-$	$XeF^+Sb_2F_{11}^-$ [a]	Assignment
624 (100)	619 (100)	ν(Ng–F)
262 (6)	269 (11)	ν(Ng- - -F)
153 (sh)	180 (4)	δ(F–Ng- - -F)
145 (4)	127 (37)	
127 (1)		
478 (7)	484 (7)	ν(Sb- - -F–Ng)
702 (3)		
688 (3)	688 (48)	$Sb_2F_{11}^-$
675 (15)	678 (8)	
657 (4)	669 (9)	
648 (26)	651 (39)	
600 (3)	603 (<1)	
591 (10)	528 (16)	
342 (1)		
313 (1)		
297 (4)	293 (8)	
226 (5)	226 (12)	
201 (1)	212 (5)	

[a] Reference 8.

due to a distortion of the octahedral anion by the formation of a fluorine bridge. The existence of such a fluorine bridge has been clearly established by x-ray crystallography[6] in the case of $XeF^+Sb_2F_{11}^-$ and similar fluorine bridges have been found in many other related compounds.

For the linear F–Kr---F group, three modes are expected, the Kr–F stretching mode, the Kr---F stretching mode, and the doubly degenerate F–Kr---F bending mode, all of which are active in the Raman spectrum. In a recent study,[8] ν(Xe–F), ν(Xe---F), and δ(F–Xe---F) have been assigned in the $XeF^+SbF_6^-$ and $XeF^+AsF_6^-$ compounds. Similar assignments can be made for the $KrF^+MF_6^-$ salts and the Kr–F and Kr---F stretching modes have frequencies that are remarkably close to the corresponding frequencies for the Xe–F^+ compounds (Table II).

As an initial assumption, the anion in structure II can be

$$\text{F–Kr}^+\text{- - -F–MF}_5$$
II

regarded as distorted from O_h to C_{4v} symmetry. The correlation between O_h and C_{4v} symmetries is given in Table IV.

Table IV. Approximate Descriptions of Vibrational Modes and Correlations for MF_6 Molecules with O_h and C_{4v} Symmetry

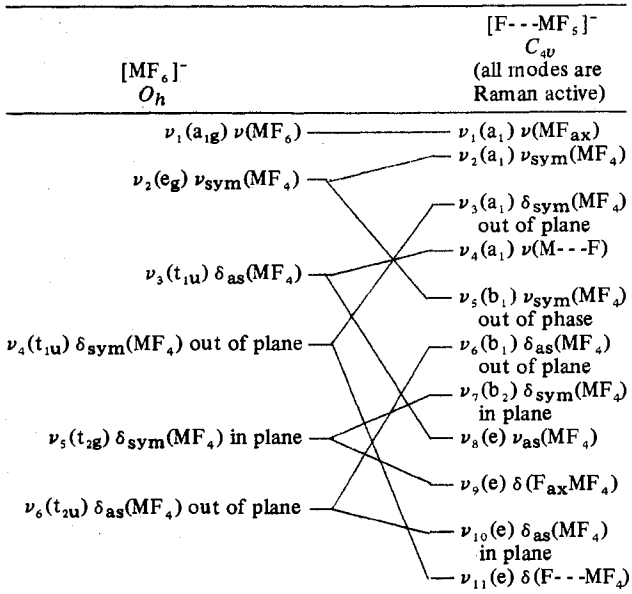

As in the cases of $Xe_2F_3^+$,[14] $XeF^+Sb_2F_{11}^-$,[6] and $XeF^+RuF_6^-$,[24] the Kr---F---M bridge angle is likely to be significantly less than 180°; however, this is not expected to cause a significant deviation from C_{4v} symmetry because of the remoteness of the ---F–MF_5 group from the Kr–F part of the complex. The further splitting of the e modes, which is expected under C_{3v} or other lower symmetry, was, in any case, not observed.

Since the ---F–MF_5 group is expected to have bond angles close to 90° and M–F bond lengths similar to those of the undistorted MF_6^- anions, the assignment of observed frequencies can be guided, to a considerable extent, by comparison with the observed frequencies of the NO^+ [7,25] and alkali metal salts[25] of the octahedral anions as well as by the data for a number of MF_5X-type C_{4v} model compounds and their octahedral MF_6 parent compounds[26] listed in Table V. In the majority of the model compounds the central atom is of similar or identical mass to the central atom in the distorted MF_6^- anion. All 11 modes of the C_{4v} molecules are active in the

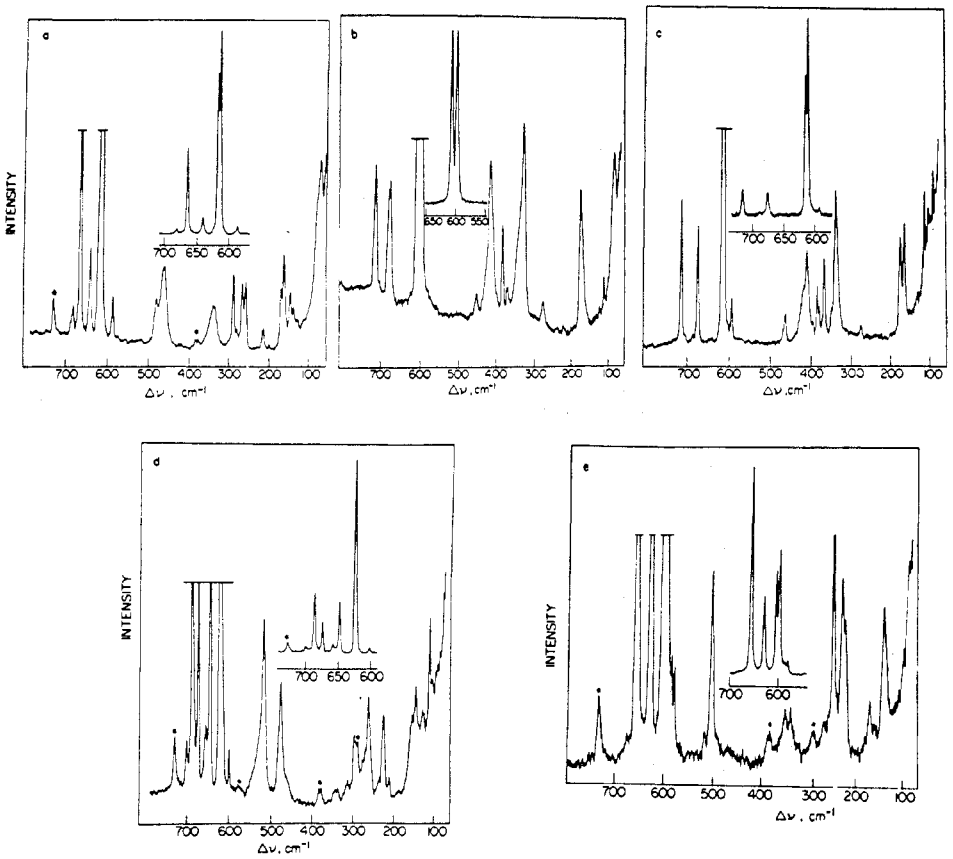

Figure 2. Low-temperature (−90°C) Raman spectra of (a) $KrF^+SbF_6^-$, (b) α-$KrF^+AsF_6^-$, (c) β-$KrF^+AsF_6^-$, (d) $KrF^+Sb_2F_{11}^-$, (e) $KrF^+PtF_6^-$. Asterisks denote lines arising from the FEP sample tube.

Table V. Vibrational Frequencies for Some MF_5X and MF_6 Species

Frequency (cm^{-1})										
TeF_5Cl[a]	TeF_6[b]		$H_3O^+SbF_5OH^-$[c]		$SbF_5 \cdot H_2O$[c]		$SbF_5 \cdot SO_2$[d]	$K^+SbF_6^-$[e]		Assignment	
R	R	Ir	R	Ir	R	Ir	R	R	Ir	C_{4v}	O_h
712 (20)	697		655 (s)	640 (s)	645 (s)	638 (sh)	643 (56)	661 (vs)		$\nu_1(a_1)$	$\nu_1(a_{1g})$
660 (100) ~660	670		582 (m) 566 (m)	570 (sh) *j*	585 (m) 556 (w)	570 (sh) 558 (w) *j*	597 (21) 540 (10)	575 (s)		$\nu_2(a_1)$ $\nu_5(b_1)$	$\nu_2(e_g)$
410 (49) 727 (sh, ~6)		752	470 (m) 670 (s)	470 (w)	488 (m) 677 (s)	498 (w) 655 (s)	519 (7) 661 (100)		655 (vs)	$\nu_4(a_1)$ $\nu_8(e)$	$\nu_3(t_{1u})$
313 (5) 212 (1)		325	266 (sh)	275 (w) 230 (m)	278 (w) 252 (sh)	265 (w) 225 (w) 210 (sh)	258 (6) 231 (13)		270 (s)	$\nu_3(a_1)$ $\nu_{11}(e)$	$\nu_4(t_{1u})$
327 (5) 260 (7)	314		285 (w)	*j*		*j* 285 (sh)	291 (14)	298 (m) 278 (m)		$\nu_7(b_2)$ $\nu_9(e)$	$\nu_5(t_{2g})$
170 (8) 304 (4)	197[i]			*j*	317 (w)	*j* 325 (w)	198 (6) 312 (7)	173[i]		$\nu_6(b_1)$ $\nu_{10}(e)$	$\nu_6(t_{2u})$
SF_5Cl[f]	SF_6[b]		SeF_5Cl[f]	SeF_6[b]	$K^+AsF_6^-$[e]		WF_5Cl[g]	WF_6[b]		$NO^+PtF_6^-$[h]		
R	R	Ir	R	R	Ir	R	Ir	R	R	Ir	R	C_{4v}	O_h
883 (2)	774		721 (8)	707		692 (s)		744 (vs)	771		647 (100)	$\nu_1(a_1)$	$\nu_1(a_{1g})$
704 (30) 625 (7)	642		656 (100) 636 (6)	659		580 (m)		703 (m) 644 (w)	677		572 (28) 590 (9)	$\nu_2(a_1)$ $\nu_5(b_1)$	$\nu_2(e_g)$
403 (100) 927 (2)		939	385 (85) 745 (3)		780		698 (vs)	407 (s) 661 (m)		711		$\nu_4(a_1)$ $\nu_8(e)$	$\nu_3(t_{1u})$
603 (2) 287[k]		614	443 (22) 213 (14)		437		382 (sh)	257 (w) 227 (w)		258		$\nu_3(a_1)$ $\nu_{11}(e)$	$\nu_4(t_{1u})$
505 (2) 584 (<1)	525		380 (~20) 424 (4)	405		375 (m)		377 (m) 290 (w)	320		249 (37) 236 (17)	$\nu_7(b_2)$ $\nu_9(e)$	$\nu_5(t_{2g})$
271 (6) 442 (8)		347[i]	336 (12)		264[i]		229[i]	182 (w) 307 (m)		127[i]		$\nu_6(b_1)$ $\nu_{10}(e)$	

[a] C. Lau and J. Passmore, unpublished results. [b] Reference 26 and references therein. [c] B. Bonnet, Thesis, Université des Sciences et Techniques du Languedoc, Montpellier, France, 1973. [d] J. Ballard and T. Birchall, private communication. [e] Reference 25. [f] K. O. Christe, C. J. Schack, and E. C. Curtis, *Inorg. Chem.*, **11**, 583 (1972), and references therein. [g] D. M. Adams, G. W. Fraser, D. M. Morris, and R. D. Peacock, *J. Chem. Soc. A*, 1131 (1968). [h] Reference 7. [i] Formally infrared and Raman inactive; the value given is the calculated frequency. [j] Infrared inactive. [k] Not observed in the Raman spectrum; the value given is the infrared frequency.

Raman spectrum. The normal modes, $\nu_1(a_1)$, $\nu_2(a_2)$, $\nu_3(a_1)$, $\nu_6(b_1)$, $\nu_7(b_1)$, and $\nu_8(e)$, involve mostly fluorine motions that are similar to corresponding motions in the O_h molecules, and a close correspondence in frequency is expected. Table II lists the assignments for the $KrF^+MF_6^-$ salts and their xenon analogues. The spectra of the XeF^+ salts have not previously been assigned on the basis of C_{4v} symmetry for the anion, but Table II shows that this may be done in a very satisfactory way and there is excellent agreement between the KrF^+ and XeF^+ compounds.

The observation of split bands arising from $\nu_2(e_g)$ and $\nu_5(t_{2g})$ does not, in itself, offer unambiguous proof for distortion of the anion by a fluorine-bridge interaction with the KrF^+ cation as these splittings could equally well arise from a simple site symmetry or factor-group splitting of these modes. The observation of derivatives of the formally forbidden $\nu_3(t_{1u})$ and $\nu_4(t_{1u})$ modes, namely $\nu_4(a_1)$, $\nu_8(e)$, $\nu_3(a_1)$, and $\nu_{11}(e)$ under C_{4v} symmetry, is, however, of particular interest. The derivatives $\nu_4(a_1)$ and $\nu_{11}(e)$ are described as ν(M---F) and δ(F---MF_4), respectively, and are of significance since they are directly associated with the fluorine-bridge interaction. The weak band that has been observed at 501–450 cm^{-1} in all of the AsF_6^-, SbF_6^-, IrF_6^-, and PtF_6^- salts of XeF^+ and KrF^+ except $XeF^+PtF_6^-$ is attributed to the bridging M---F stretch. The stretching frequency of the M---F bridge bond is significantly lower by ca. 150–250 cm^{-1} than $\nu_1(a_{1g})$ in the undistorted anion. This is consistent with the expected weakening and lengthening of this bond on bridge formation. The assignment of the F---MF_4 bend, which is derived from $\nu_4(t_{1u})$, is not completely unambiguous, but a reasonable assignment of this mode can be given in some cases.

Several workers[9,27] have recently repeated Selig and Peacock's original preparation of $KrF^+Sb_2F_{11}^-$.[4] However, the vibrational data reported by these workers on this compound are sparse and, moreover, their samples appear to have been contaminated with significant quantities of $KrF^+SbF_6^-$. We have prepared $KrF^+Sb_2F_{11}^-$ and its Raman spectrum is given in Table III along with that of the xenon analogue. The purity of the compound was confirmed by the absence of the strong lines arising from the Kr–F stretching mode of $KrF^+SbF_6^-$ at 615 and 619 cm^{-1}. Although a complete assignment of the frequencies of the $Sb_2F_{11}^-$ anion has not been made, there is generally good agreement with the anion frequencies observed for $XeF^+Sb_2F_{11}^-$ (Table III), and it seems reasonable to assume that $KrF^+Sb_2F_{11}^-$, like $XeF^+Sb_2F_{11}^-$,[6] has the cis-bridged structure III. As in the case of the MF_6^-

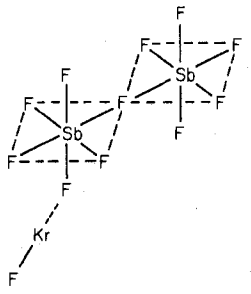

III

compounds, the observed vibrational frequencies associated with the F–Kr---F group are very close to those of the corresponding xenon compound. In both $XeF^+Sb_2F_{11}^-$ and $KrF^+Sb_2F_{11}^-$ the Ng–F stretching frequency is the highest observed for any XeF^+ or KrF^+ compound and the Ng---F stretching frequency is the lowest.

In summary, the observation of the derivatives of the formally forbidden $\nu_3(t_{1u})$ and $\nu_4(t_{1u})$ modes in the Raman spectra of the MF_6^- salts supports the view that the MF_6^- anion is distorted in these compounds. The complete anion

Table VI. Valence Stretching Force Constants and Bond Lengths of Some Noble Gas Fluorides and Fluorocations

Species	f_{X-F}, mdyn/Å	r(X–F), Å
XeF^+	3.75[a]	1.84[b]
XeF_2	2.83[c]	1.98[d]
KrF^+	3.55[a]	
KrF_2	2.46[c]	1.89[e]

[a] This work. Calculated using the Ng–F stretching frequency for the compounds $KrF^+Sb_2F_{11}^-$ and $XeF^+Sb_2F_{11}^-$, which presumably have the weakest cation–anion fluorine-bridge interaction. [b] Reference 6. [c] H. H. Claassen, G. L. Goodman, J. G. Malm, and F. Schreiner, *J. Chem. Phys.*, 42, 1729 (1965). [d] H. A. Levy and P. A. Argon, *J. Am. Chem. Soc.*, 85, 241 (1963). [e] Reference 3.

spectrum can, in fact, be satisfactorily assigned on the basis of C_{4v} rather than O_h symmetry. Moreover, the observation of modes assigned to ν(Kr---F) and δ(F–Kr---F) in both the MF_6^- and $Sb_2F_{11}^-$ compounds further supports our supposition that the origin of the distortion is a fluorine-bridge interaction with the cation. This interaction may be described as weak covalent bonding and the simple ionic formulations $KrF^+MF_6^-$ and $KrF^+Sb_2F_{11}^-$ are therefore not completely satisfactory. A description in terms of the following resonance structures seems more appropriate with the contribution from IVa being greater than that from IVb

$$\underset{\text{IVa}}{F\text{-}Kr^+\ F\text{-}MF_5^-} \qquad \underset{\text{IVb}}{F\text{-}Kr\text{-}F\ MF_5}$$

Valence Stretching Force Constants of KrF^+ and XeF^+. A comparison of the calculated force constants and bond lengths for XeF^+, KrF^+, XeF_2, and KrF_2 is given in Table VI. Values for the NgF^+ cations were calculated from the stretching frequency observed in the $Sb_2F_{11}^-$ salts, assuming them to be simple isolated diatomic molecules. A consideration of the Raman spectroscopic data[7,8] and the x-ray crystal structures of $XeF^+Sb_2F_{11}^-$[6] and $XeF^+RuF_6^-$[24] shows that the fluorine-bridge interaction in $XeF^+Sb_2F_{11}^-$ is the weakest of all the reported XeF^+ compounds. The present Raman spectroscopic study indicates that the fluorine bridge with the $Sb_2F_{11}^-$ anion is correspondingly weak in $KrF^+Sb_2F_{11}^-$. The NgF^+ cations in the $Sb_2F_{11}^-$ salts can, therefore, be regarded as most closely approximating free NgF^+ cations.

Several observations may be made on the data presented in Table VI. First, we note that the NgF^+ cations have higher stretching force constants than in the neutral NgF_2 molecule and in the case of XeF^+ the bond length is also correspondingly shorter. This is consistent with the view that the two structures Va and Vb make a considerable contribution to the bonding

$$\underset{\text{Va}}{F\text{-}\overset{+}{N}g\ \overset{-}{F}} \qquad \underset{\text{Vb}}{\overset{-}{F}\ \overset{+}{N}g\text{-}F}$$

in a noble gas difluoride. Thus the bond order is lower than in the cation which can be reasonably represented by the single structure F–Ng^+. The KrF stretching force constant is lower than the XeF stretching force constant in both the NgF^+ ions and the NgF_2 molecules. It seems probable that KrF bonds are generally weaker than the corresponding XeF bonds. The KrF^+ bond length has not yet been measured but it seems likely that it will be longer than the value of 1.75 Å predicted by an ab inito calculation[23] and from a consideration of the force constants and bond lengths in Table VI a value of approximately 1.80 Å may be predicted.

$Kr_2F_3^+SbF_6^-$ and $Kr_2F_3^+AsF_6^-$. The Raman spectra of $Kr_2F_3^+SbF_6^-$ and $Kr_2F_3^+AsF_6^-$ (Figure 3) show the expected anion frequencies. The Raman spectrum of the cation may be interpreted on the basis of C_{2v} symmetry for the symmetrical angular molecule I for which nine normal modes are expected, 7 a and 2 a'', all of which are active in the Raman spectrum. Of these nine modes only the four stretching modes

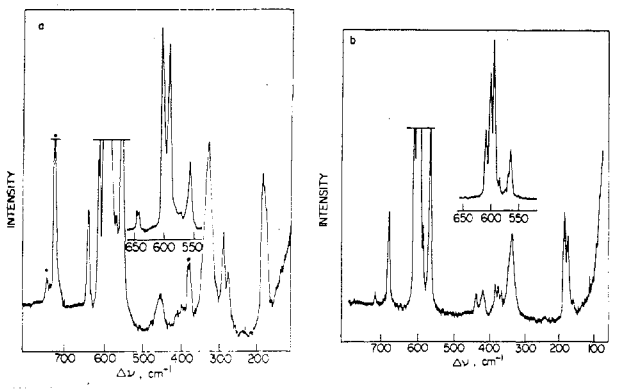

Figure 3. The Raman spectra (−90°C) of (a) $Kr_2F_3^+SbF_6^-$ and (b) $Kr_2F_3^+AsF_6^-$. Asterisks denote lines arising from the FEP sample tube.

Table VII. The Correlation for the Site Groups $C_{\infty v}$ and C_s to the Molecular Symmetry $D_{\infty h}$ of KrF_2

$D_{\infty h}$[a] F-Kr-F	$C_{\infty v}$[b] ---F---Kr-F	C_s[b] F---Kr-F
$\nu_1(\Sigma_g^+)$	$\nu_1(\Sigma^+)$	$\nu_1(a')$
$\nu_2(\Pi_u)$	$\nu_2(\Sigma^+)$	$\nu_2(a')$
$\nu_3(\Sigma_u^+)$	$\nu_3(\Pi)$	$\nu_3(a')$, $\nu_4(a'')$

[a] ν_1 is Raman active and ν_2 and ν_3 are infrared active. [b] All modes are both Raman and infrared active.

ν_1 to ν_4 can be assigned with any confidence (Table VIII). These stretching modes have quite similar frequencies to those found previously for the $Xe_2F_3^+$ cation[8] and their most noteworthy feature is that the splitting between the in-phase and out-of-phase motions is considerably greater than was observed for $Xe_2F_3^+$. This would appear to indicate that the bond angle at the bridging fluorine is larger in $Kr_2F_3^+$ than in $Xe_2F_3^+$ and/or that there is a greater coupling between the two halves of the molecule than in $Xe_2F_3^+$. Four bands with frequencies between 158 and 238 cm^{-1} in $Kr_2F_3^+AsF_6^-$ and three bands between 176 and 186 cm^{-1} in $Kr_2F_3^+SbF_6^-$ may be attributed to the bending modes in the molecule.

An alternative explanation of the rather large difference in the stretching frequencies of $Kr_2F_3^+$ would be that the cation is unsymmetrical (VI) in the solid state although it is clearly

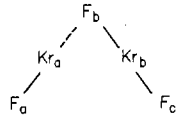

VI

shown, by our NMR results, to be symmetrical in solution. In this case there will be one short and strong Kr–F_a bond and one rather weaker and longer Kr–F_b bond and a similar difference in the two Kr---F_b bridging bonds. In this case the 603, 594 cm^{-1} band of $Kr_2F_3^+SbF_6^-$ would be assigned to the stronger Kr–F_a bond and the 555 cm^{-1} band to the weaker Kr–F_b bond.[28] Similarly the bands at 456 and 330 cm^{-1} are assigned to the two bridging bonds.

An alternative method of interpreting the spectrum on the assumption that the ion has the asymmetric structure (VI) is to regard it as a distorted KrF_2 molecular fluorine bridged to a KrF^+ ion. One of the Kr–F bonds in KrF_2 is elongated by the formation of the fluorine bridge and the other is correspondingly shortened and the $D_{\infty h}$ symmetry of the KrF_2 molecule is effectively lowered to $C_{\infty v}$ or lower symmetry. The correlation diagram for $D_{\infty h}$, $C_{\infty v}$, and C_s symmetries is given in Table VII. The bands observed at 555, 567 cm^{-1} at 437, 456 cm^{-1} and at 183, 186 cm^{-1} are assigned to $\nu_1(\Sigma^+)$, $\nu_2(\Sigma^+)$, and $\nu_3(\Pi)$ of KrF_2, respectively, under $C_{\infty h}$ symmetry. The

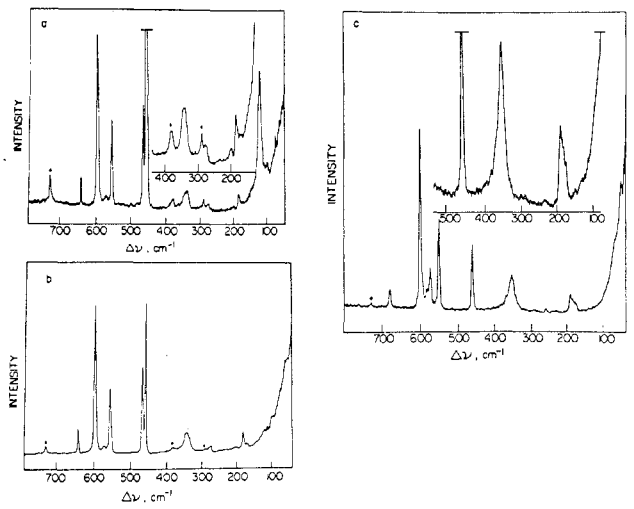

Figure 4. The Raman spectra (−90°C) of (a) $Kr_2F_3^+ \cdot x KrF_2 \cdot SbF_6^-$ plus a large excess of KrF_2; (b) $Kr_2F_3^+ \cdot x KrF_2 \cdot SbF_6^-$ plus a slight excess of KrF_2; (c) $Kr_2F_3^+ \cdot x KrF_2 \cdot AsF_6^-$ plus a slight excess of KrF_2. Asterisks denote line arising from the FEP sample tube.

observation of the formally forbidden $\nu_2(\Pi_u)$ and $\nu_3(\Sigma_u^+)$ modes of KrF_2 in the Raman spectrum is consistent with a lowering of the $D_{\infty h}$ symmetry of the molecule by a fluorine-bridge interaction with the KrF^+ ion.

Some further evidence that the $Kr_2F_3^+$ ion may be asymmetric in the solid state is provided by the spectrum of the AsF_6^- ion which shows several additional bands that may be assigned as arising from the distortion of the "octahedral" ion to C_{4v} symmetry. Thus bands at 347, 418, and 718 cm^{-1} have very similar frequencies to similar bands observed in the AsF_6^- part of the spectrum of $KrF^+AsF_6^-$ and they may be assigned as $\nu_7(b_2)$, $\nu_3(a_1)$, and $\nu_8(e)$, respectively. As in the case of $KrF^+AsF_6^-$ it is reasonable to assume that this lowering of the symmetry of the AsF_6^- ion is due to fluorine-bridge formation. Such a fluorine bridge between AsF_6^- and $Kr_2F_3^+$ would inevitably lead to a distortion of the $Kr_2F_3^+$ to an unsymmetrical form. It must be admitted, however, that similar additional bands were not observed in the spectrum of SbF_6^- nor has similar fluorine bridging, in which the noble gas atom acquires a coordination number of greater than two, been observed in any similar xenon(II) compounds.

On adding KrF_2 to $Kr_2F_3^+AsF_6^-$ appreciable changes occur in the spectrum, some bands change in intensity and others shift somewhat in frequency (Table VIII). These changes are not simply due to excess KrF_2 but appear to indicate the formation of a new compound. Nevertheless the spectrum remains quite similar to that of $Kr_2F_3^+$ and the structure of this new species is presumably closely related to that of $Kr_2F_3^+$. For the present it can only be formulated as $Kr_2F_3^+ \cdot xKrF_2$, the simplest form of which would be $Kr_3F_5^+$.

The Question of the Purity of the $Kr_2F_3^+MF_6^-$ Salts. In view of the instability of $Kr_2F_3^+SbF_6^-$ and $Kr_2F_3^+AsF_6^-$ at room temperature, it was not possible to obtain good analyses of these salts. In addition to ^{19}F NMR spectroscopy, Raman spectroscopy has, therefore, been relied upon extensively to establish their purity.

Since both $Kr_2F_3^+SbF_6^-$ and $Kr_2F_3^+ \cdot xKrF_2 \cdot SbF_6^-$ have lines occurring at ~556 cm^{-1}, experiments were devised which would clearly show that the spectrum assigned to $Kr_2F_3^+SbF_6^-$ does not arise from a mixture of $Kr_2F_3^+SbF_6^-$ with either KrF_2 or $Kr_2F_3^+ \cdot KrF_2 \cdot SbF_6^-$. The decomposition of $Kr_2F_3^+ \cdot xKrF_2 \cdot SbF_6^-$ in the presence of an initially large excess of KrF_2 was monitored by briefly warming samples to room temperature followed by quenching of the reaction and recording the spectrum at −90° (Figure 4). Using this technique it was

Table VIII. Raman Spectra of Some $Kr_2F_3^+$ and $Kr_2F_3^+ \cdot xKrF_2$ Salts and Their Xenon Analogues

Frequency, cm^{-1} [a]				Assignment	
$Kr_2F_3^+SbF_6^-$	$Kr_2F_3^+ \cdot xKrF_2 \cdot SbF_6^-$ [b]	$Kr_2F_3^+AsF_6^-$	$Kr_2F_3^+ \cdot xKrF_2 \cdot AsF_6$	$Kr_2F_3^+$	
603 (100) 594 (89)	599 (100)	610 (43) 600 (80) 594 (100)	602 (100)	$\nu_1(a')$	$\nu(Kr_a\text{-}F_a)$
555 (34)	557 (50)	570 (4) 567 (31)	575 (23) 553 (50)	$\nu_2(a')$	$\nu(Kr_b\text{-}F_c)$
456 (4)	466 (60)[d]	437 (5)	462[e]	$\nu_3(a')$	$\nu(Kr_b\text{- - -}F_b)$
330 (18)	340 (14)	347 (sh) 336 (17)	355 (19)	$\nu_4(a')$	$\nu(Kr_a\text{- - -}F_b)$
186 (16) 180 (sh) 176 (sh)	200 (2) 188 (10) 122 (46)	239 (1) 183 (15) 174 (13) 158 (2)	190 (10) 184 (sh) 177 (sh)	$\nu_5(a'), \nu_8(a'')$ $\nu_6(a'), \nu_9(a'')$ $\nu_7(a')$	$\delta(F\text{-}Kr\text{- - -}F)$
645 (10) 642 (9) 572 (2)	642 (16) 572 (5)	678 (12) 585 (5) 718 (1) 418 (6) 384 (5)	682 (10) 585 (5)	$\nu_1(a_{1g})$ $\nu_2(e_g)$ $\nu_3(t_{1u})$	MF_6^-
289 (10) 277 (16)	289 (8) 278 (5)	376 (4) 366 (4)	371 (sh)	$\nu_5(t_{2g})$	
$Xe_2F_3^+SbF_6^-$ [c]		$Xe_2F_3^+AsF_6^-$ [c]			
591 (66) 582 (100)		598 (95) 588 (100)		$\nu(Xe\text{-}F)$	
420 (<1)		417 (<1) 401 (<1)		$\nu(Se\text{- - -}F)$	
179 (6) 171 (15) 161 (21)		163 (5)		$\delta(F\text{-}Xe\text{- - -}F)$	
645 (24)		678 (20) 667 (4)		$\nu_1(a_{1g})$	
		580 (sh)		$\nu_2(e_g)$	MF_6^-
296 (2) 293 (2) 282 (12)		367 (7)		$\nu_5(t_{2g})$	
255 (<1)		255 (5)			

[a] Spectra of all of the $Kr_2F_3^+$ salts were recorded at −90° in FEP sample tubes. Lines due to FEP have been deleted from the spectra. The spectra of $Kr_2F_3^+AsF_6^-$ and $Kr_2F_3^+ \cdot xKrF_2 \cdot AsF_6^-$ were also recorded at −90° in glass sample tubes. [b] Data given are for the spectrum depicted in Figure 4a. The strong line at 122 cm^{-1} is only visible when a large excess of KrF_2 is present (cf. Figures 4a and 4b). [c] Reference 8. [d] A strong line due to $\nu_1(\Sigma_g^+)$ of excess KrF_2, also present in some of these preparations, was also observed at 456 cm^{-1}. [e] The line due to $\nu_1(\Sigma_g^+)$ of free KrF_2, also present in these preparations, is presumably coincident with $\nu_3(a')$ of $Kr_2F_3^+$.

possible to monitor the initial decrease and eventual disappearance of the line due to free KrF_2 to give $Kr_2F_3^+ \cdot xKrF_2 \cdot SbF_6^-$ (Scheme I). Lines due to $Kr_2F_3^+SbF_6^-$ next emerged, including the 555-cm^{-1} line which was nearly coincident with the 557-cm^{-1} line of $Kr_2F_3^+ \cdot xKrF_2 \cdot SbF_6^-$. It is particularly important to note that the intense line at 466 cm^{-1} arising from $Kr_2F_3^+ \cdot xKrF_2 \cdot SbF_6^-$ decreased simultaneously with the rest of the spectrum of this species as lines due to $Kr_2F_3^+SbF_6^-$ emerged and eventually replaced the lines due to the $Kr_2F_3^+ \cdot xKrF_2$ salt.

The decomposition of $Kr_2F_3^+SbF_6^-$ to $KrF^+SbF_6^-$ (Scheme I) was also monitored by this technique. The decomposition led directly to $KrF^+SbF_6^-$ and showed that the 555-cm^{-1} line decreased simultaneously with the rest of the $Kr_2F_3^+SbF_6^-$ spectrum as the $KrF^+SbF_6^-$ spectrum grew in intensity.

In a related experiment with $Kr_2F_3^+AsF_6^-$, which has a similar intense band at 567 cm^{-1}, it was shown that in the presence of liquid AsF_5 at −63° this band also decreased with the remainder of the $Kr_2F_3^+AsF_6^-$ spectrum, leading directly to β-$KrF^+AsF_6^-$ with no intermediate species being formed (Scheme II).

The absence of lines assignable to KrF_2, $KrF^+MF_6^-$, or $Kr_2F_3^+ \cdot xKrF_2 \cdot MF_6^-$ (M = As or Sb) strongly supports the view that the Raman spectra assigned to the $Kr_2F_3^+MF_6^-$ compounds are those of the pure compound. In addition, the reaction chemistry described above in Schemes I and II is consistent with this view in that no intermediate species were observed in the Raman spectra of these phases on going from $Kr_2F_3^+ \cdot xKrF_2$ to $Kr_2F_3^+$ to KrF^+.

Experimental Section

Materials. Krypton difluoride was prepared by passing an electrical discharge through a mixture of krypton (Matheson) and fluorine (Matheson) at liquid nitrogen temperature (−183°). The method was similar to that described previously by Schreiner et al.[2]

Antimony pentafluoride (Ozark-Mahoning Co.) was purified by double distillation in an atmosphere of dry nitrogen, using an all-glass apparatus, and stored in glass vessels in a drybox. The distillation apparatus and procedure is described elsewhere.[29] The boiling point of the distilled material was 142 to 143°.

Arsenic pentafluoride (Ozark-Mahoning Co.) was used without further purification.

Anhydrous hydrogen fluoride (Harshaw Chemical Co.) was purified by fractional distillation. A Kel-F distillation column similar to that described by Shamir and Netzer[30] was used. In the present work, HF having a specific conductance of 1×10^{-4} Ω^{-1} at 25° was routinely obtained. This corresponds to a water concentration of ca. 1×10^{-4} *m*.

Bromine pentafluoride (Matheson) was distilled into a Kel-F trap fitted with Teflon valves and purified by passing fluorine at atmospheric pressure through the liquid until all the Br_2 and BrF_3 had reacted. After degassing several times, HF was removed by distilling the BrF_5 onto dry sodium fluoride in a Kel-F tube and allowing it to stand at room temperature under 1 atm of fluorine until used.

Platinum hexafluoride (Ozark-Mahoning Co.) was used without further purification. Owing to its photo-sensitivity, all manipulations involving PtF_6 were carried out in an all-Teflon and FEP apparatus

under subdued lighting conditions.

Oxygen gas (Canadian Liquid Air) containing less than 10 ppm H_2O and xenon (Matheson), 99.9%, were used in the reactions with KrF^+.

Sodium fluoride (Mallinckrodt), 99.9%, was dried at 200° under vacuum in a glass tube for 2–3 days and stored under an atmosphere of dry nitrogen until used.

Preparation of Salts of KrF^+, $Kr_2F_3^+$, and $Kr_2F_3^+ \cdot xKrF_2$ Cations. The krypton(II) salts are extremely potent oxidants and readily oxidize oxygen gas to O_2^+; consequently all of these compounds were stored under a positive pressure (1.7 atm) of high purity argon gas at −78°. The low-temperature Raman spectra (−90°) were relied upon extensively to demonstrate the purities of these compounds. The homogeneity of each preparation was verified by recording the spectrum at a minimum of three points along the length of the sample region of the reaction tube.

A number of reactions which liberate F_2 gas at low temperatures (−78 to 25°) have been investigated in the course of this work. That fluorine was indeed liberated in these reactions has been unequivocally established by its characteristic yellow-orange gas discharge. The discharge was excited by means of a Tesla coil on the vacuum pump side of a glass liquid nitrogen cold trap as noncondensable gases from the reaction vessel, also cooled to −196°, were pumped off.

$KrF^+Sb_2F_{11}^-$, $KrF^+SbF_6^-$, $Kr_2F_3^+SbF_6^-$, and $Kr_2F_3^+ \cdot xKrF_2 \cdot SbF_6^-$. The 1:2 adduct of KrF_2 with SbF_5, $KrF^+Sb_2F_{11}^-$, was prepared by condensing 0.09 g (0.75 mmol) of KrF_2 onto 1.0 g (4.4 mmol) of SbF_5 in an FEP tube. The adduct was only partially soluble at room temperature and slowly decomposed evolving Kr and F_2 gases. Similar behavior was also noted by Selig and Peacock[4] who first prepared and analyzed $KrF^+Sb_2F_{11}^-$. Excess SbF_5 was immediately pumped off at room temperature and the purity of the adduct was confirmed by the absence of lines at 619 and 615 cm^{-1} due to the Kr–F stretching mode of $KrF^+SbF_6^-$ in the low-temperature Raman spectrum.

The 1:1 adduct of SbF_5 with KrF_2 was prepared by three different routes. In one case, excess KrF_2 was condensed onto $KrF^+Sb_2F_{11}^-$ in an FEP tube at −196°. The reaction mixture was allowed to warm up to and stand at 0° for 0.5 hr. Brief warming of the vessel and contents to room temperature ensured that the reaction was complete. When the ratio KrF_2:SbF_5 was significantly greater then 2:1, brief warming to room temperature resulted in an immediate exothermic reaction in which the reactants fused and rapid evolution of Kr and F_2 gasses took place. In several instances the decomposition was accompanied by flashes of white light. After the reaction had taken place, the reaction tube and contents were cooled to 0°, and any excess of KrF_2 remaining was pumped off to yield the pure $KrF^+SbF_6^-$ salt. Continued pumping on $KrF^+SbF_6^-$ at room temperature led eventually to the appearance of Raman lines attributable to $KrF^+Sb_2F_{11}^-$. The adduct was also prepared directly by reacting excess KrF_2 with SbF_5. Finally, the adduct was obtained pure as the decomposition product of $Kr_2F_3^+SbF_6^-$ (Scheme I). The purities of the $KrF^+SbF_6^-$ preparations were confirmed by the absence of lines due to the Kr–F stretching modes of $KrF^+Sb_2F_{11}^-$ (624 cm^{-1}) and of $Kr_2F_3^+SbF_6^-$ (603, 594 and 555 cm^{-1}), which are intense in the pure compounds.

The $Kr_2F_3^+SbF_6^-$ salt was prepared by methods similar to those described for the preparation of $KrF^+SbF_6^-$, i.e., by the interaction of excess KrF_2 with $KrF^+SbF_6^-$, $KrF^+Sb_2F_{11}^-$, or SbF_5. In all cases, the KrF_2:SbF_5 ratio was greater than 3:1 and under these conditions the adduct formulated as $Kr_2F_3^+ \cdot xKrF_2 \cdot SbF_6^-$ was present in a mixture with KrF_2. The decomposition of this adduct was vigorous at room temperature and has been alluded to in the previous description of the preparation of $KrF^+SbF_6^-$. The decomposition could, however, be controlled by judicious warming and cooling of the reaction mixture in an ice bath. The correct stoichiometry was arrived at by periodically quenching the reaction at −90° and monitoring the progress of the decomposition by Raman spectroscopy at this temperature. When the last trace of $Kr_2F_3^+ \cdot xKrF_2 \cdot SbF_6^-$ had disappeared, as indicated by the disappearance of the strong line at 466 cm^{-1}, the decomposition was halted. When $Kr_2F_3^+SbF_6^-$ was carefully prepared by this technique no Raman lines arising from $KrF^+SbF_6^-$ or $Kr_2F_3^+ \cdot xKrF_2 \cdot SbF_6^-$ (strong characteristic lines at 599, 557, and 466 cm^{-1}) were evident at any point along the sample region of the reaction vessel.

α-$KrF^+AsF_6^-$, β-$KrF^+AsF_6^-$, $Kr_2F_3^+AsF_6^-$, and $Kr_2F_3^+ \cdot xKrF_2 \cdot AsF_6^-$. In each preparation ca. 0.10 g (0.8 mmol) of KrF_2 was condensed into an FEB tube at −196°. Arsenic pentafluoride, ca. 0.50 g (3.0 mmol), was condensed onto KrF_2 and the tube and contents were isolated from the main manifold and warmed to −63°. Under these conditions, AsF_5 was liquid and was in intimate contact with KrF_2. After 1 hr, the tube was again opened to the manifold and the AsF_5 was allowed to expand into the manifold while slowly warming the reaction tube and its contents to room temperature. The unreacted KrF_2 and resulting mixture of KrF^+ and $Kr_2F_3^+$ salts were allowed to stand in contact with 1.7 atm of gaseous AsF_5 for an additional 0.5 hr. Cooling to −78° and pumping off the unreacted AsF_5 indicated that a small amount of noncondensable gas (Kr and F_2) had formed due to some slight decomposition of the adduct and/or KrF_2 at room temperature. When the Raman spectrum of the resulting product was obtained immediately, the spectrum corresponded to that of the high-temperature modification α-$KrF^+AsF_6^-$. The low-temperature β modification was obtained by allowing the sample to stand at −78°. The transition was periodically monitored by Raman spectroscopy at −90° and occurred within 24 hr. At room temperature the transition of β-$KrF^+AsF_6^-$ to α-$KrF^+AsF_6^-$ was rapid and complete within 15 min.

The $Kr_2F_3^+AsF_6^-$ salt was conveniently synthesized by removing volatile heads from α-$KrF^+AsF_6^-$. In a typical preparation, a sample of α-$KrF^+AsF_6^-$ was rapidly warmed to room temperature. The Teflon valve was opened on the reaction vessel and volatiles consisting of mainly AsF_5 were allowed to expand into the evacuated manifold to give a pressure of 40 to 60 Torr. When the reaction tube was isolated and the manifold evacuated, no noncondensables were detected. The process was repeated in rapid succession as many times as necessary until only a slight pressure rise was detected, i.e., 5 to 10 Torr, and two additional heads were removed in rapid succession. The resulting product was immediately cooled to and stored at −78°. No Raman lines were visible that could be attributed to α-$KrF^+AsF_6^-$ (607 and 596 cm^{-1}) and upon standing at −78° none due to the low-temperature modification, β-$KrF^+AsF_6^-$ (619 and 615 cm^{-1}), developed.

The salt $Kr_2F_3^+ \cdot xKrF_2 \cdot AsF_6^-$ was formed by distilling excess KrF_2 either onto α-$KrF^+AsF_6^-$ or onto $Kr_2F_3^+AsF_6^-$. This compound was generally prepared with a significant amount of KrF_2 also present in the sample.

The β modification of $KrF^+AsF_6^-$ was also obtained by the reaction of liquid AsF_5 with $Kr_2F_3^+AsF_6^-$ at −63°. The reaction was monitored by Raman spectroscopy and was essentially complete after 2 days.

The syntheses of all of the AsF_5 salts of KrF_2 were subsequently repeated in Pyrex glass NMR tubes previously passivated with F_2, and no signs of attack upon the glass surface were evident. A sealed-tube reaction between KrF_2 and liquid AsF_5 at room temperature was also carried out in glass. The reaction was rapid and yielded pure α-$KrF^+AsF_6^-$ upon distillation of excess AsF_5 from the solid, which was maintained at −78°, to a portion of the tube cooled to −196°.

$KrF^+PtF_6^-$. A typical preparation consisted of condensing ca. 0.10 g (0.32 mmol) of PtF_6 from its nickel storage vessel into an FEP tube at −196°. Small additions of KrF_2 were made at −196° followed by warming to 0°. The reaction was rapid at 0° and upon cooling to −196° F_2 gas was pumped off. The reaction was judged to be complete when no red-brown PtF_6 vapor could be visually detected upon warming the vessel to room temperature. Excess KrF_2 and/or small quantities of unreacted PtF_6 were pumped off at room temperature. The resulting canary-yellow solid, $KrF^+PtF_6^-$, was stored under a positive pressure of argon gas at −78° until its Raman spectrum could be obtained.

Nuclear Magnetic Resonance Spectroscopy. Fluorine-19 NMR spectra were measured with a Varian DA-601L spectrometer operating at 56.4 or 58.3 MHz. The 2497 Hz audio modulation side bands forming part of the baseline stabilization circuitry of the instrument usually overlapped part of the centerband spectrum, and the "lock box" had therefore been modified as described elsewhere[31] to take an external manual oscillator frequency from a General Radio Co. type 1304-B beat frequency audio oscillator. In this work, the modulation frequency was 25000 Hz and spectra were usually measured using the first upper side band in field sweep unlock mode. The spectra were calibrated by the usual audio side band method using a Muirhead-Wigan D-890-A decade oscillator. Side band frequencies were checked with a General Radio type 1191 frequency counter. All spectra were referenced with respect to external $CFCl_3$ by sample tube interchange. The chemical shifts are estimated to be accurate to ±0.5 ppm.

Variable-temperature spectra were obtained using a Varian V4540 temperature controller with a variable temperature probe. The sample tube temperature was determined by insertion of a copper–constantan

thermocouple encased in a thin-walled NMR tube into the sample region of the probe.

Laser Raman Spectroscopy. A Spectra Physics Model 164 argon ion laser giving up to 900 mW at 5145 Å or a Spectra Physics Model 125 helium–neon laser with an output of 50 mW at 6328 Å was used to excite the spectra. The spectrometer was a Spex Industries Model 1400 3/4-meter Czerny-Turner double monochromator equipped with gratings of 1200 grooves/mm and blazed for 7500 Å. Slit widths depended on the scattering efficiency of the sample, laser powder, etc., with 90–100 μ being typical. An I.T.T. FW 130 phototube detector in conjunction with a pulse count system consisting of pulse amplifier, analyzer, and ratemeter (Hamner NA-11, NC-11, and N-780A, respectively) and a Texas Instruments FS02WBA strip chart recorder were used to record the spectra. The spectrometer was periodically calibrated by recording the discharge lines from an argon lamp over the spectral range of interest; the Raman shifts quoted are estimated to be accurate to ± 2 cm^{-1}.

Sample tubes were mounted at right angles to the laser beam and Raman-scattered radiation was observed perpendicular to both these directions.

Low-temperature spectra were recorded by mounting the sample in a double-walled Pyrex glass Dewar silvered except for a centimeter wide band around the center through which exciting radiation entered and scattered radiation was observed. Liquid nitrogen was boiled off from a Dewar at a controlled rate by an electric heater and the cold gas passed through the sample Dewar. The temperature was monitored with a copper–constantan thermocouple positioned just upstream of the sample region.

Sample Preparation. All sample tubes were interchangeable and were used for either Raman or NMR work. Preparative work was carried out in 3.91-mm o.d. (0.31-mm wall) lengths of Teflon FEP spaghetti tubing heat sealed at one end and connected through a 45° SAE flare to a Teflon adaptor. Krypton difluoride–arsenic pentafluoride systems were also handled in 5-mm o.d. heavy wall precision polished glass NMR tubes glass blown onto lengths of 0.25-in. o.d. glass tubing. Sample tubes were attached to Teflon valves by means of standard 0.25-in. Teflon Swagelok compression fittings, dried under vacuum and passivated with F_2 prior to use.

Hydrogen fluoride and BrF_5 were distilled directly from their storage vessels into sample tubes through an inert fluoroplastic system. Antimony pentafluoride was added in a drybox using a glass hypodermic syringe. Samples of KrF^+ and $Kr_2F_3^+$ salts were prepared directly in the FEP sample tube and the appropriate solvent for NMR solution studies was distilled in under vacuum.

Samples for ^{19}F NMR were not spun, and frequently, in the case of fluoroplastic tubes, the Teflon valve assembly was left attached. FEP sample tubes were inserted into a thin-walled glass NMR tube, which was then placed in the NMR probe.

Raman spectra were obtained exclusively in either FEP or glass sample tubes. The spectrum of the FEP sample tube was nearly always observed, and in observing different samples at −90° the intensities of the FEP lines relative to each other remained constant. Their prominence in the overall spectrum, however, depended on the efficiency of the sample as a Raman scatterer. Lines arising from FEP and glass have been subtracted out of the spectra reported in the tables but not in the figures.

The compound, $KrF^+PtF_6^-$, is highly colored (canary-yellow) and was found to absorb strongly enough in both the red (6328 Å) and the green (5145 Å) laser beams to cause decomposition at temperatures as low as −110°. Since the compound has no appreciable solubility in anhydrous HF at −70° the problem of decomposition was overcome by obtaining the spectrum of the solid under a layer of liquid HF at −70° using the 6328 Å lines. Hydrogen fluoride, which has no lines in the spectral region of interest, serves as an effective thermal sink at this temperature, thus preventing localized heating and decomposition of the $KrF^+PtF_6^-$ in the laser beam.

Registry No. $KrF^+Sb_2F_{11}^-$, 39578-36-4; $KrF^+SbF_6^-$, 52708-44-8; $Kr_2F_3^+SbF_6^-$, 52721-22-9; $KrF^+AsF_6^-$, 50859-36-4; $Kr_2F_3^+AsF_6^-$, 52721-23-0; $KrF^+PtF_6^-$, 56929-92-1; KrF_2, 13773-81-4; SbF_5, 7783-70-2; AsF_5, 7784-36-3; PtF_6, 13693-05-5.

References and Notes

(1) Presented in part at the Assemblée generale annuelle de la Societé Chimique de France, Marseille, France, May 23–25, 1973; the Second Winter A.C.S. Fluorine Conference, St. Petersburg, Fla, Feb 3–8, 1974, and the 5th European Symposium on Fluorine Chemistry, Aviemore, Scotland, Sept 16–20, 1974.
(2) F. Schreiner, J. G. Malm, and J. S. Hindman, *J. Am. Chem. Soc.*, **87**, 25 (1965).
(3) R. D. Burbank, W. E. Falconer, and W. A. Sunder, *Science*, **178**, 1285 (1972).
(4) H. Selig and R. D. Peacock, *J. Am. Chem. Soc.*, **86**, 3895 (1964).
(5) D. E. McKee, C. J. Adams, A. Zalkin, and N. Bartlett, *J. Chem. Soc., Chem. Commun.*, 26 (1973).
(6) V. M. McRae, R. D. Peacock, and D. R. Russell, *Chem. Commun.*, 62 (1969).
(7) F. O. Sladky, P. A. Bulliner, and N. Bartlett, *J. Chem. Soc. A*, 2179 (1969).
(8) R. J. Gillespie and B. Landa, *Inorg. Chem.*, **12**, 1383 (1973).
(9) B. Frlec and J. H. Holloway, *J. Chem. Soc., Chem. Commun.*, 370 (1973).
(10) R. J. Gillespie and G. J. Schrobilgen, *J. Chem. Soc., Chem. Commun.*, 90 (1974).
(11) B. Frlec and J. H. Holloway, *J. Chem. Soc., Chem. Commun.*, 89 (1974).
(12) B. Frlec and J. H. Holloway, *Inorg. Chem.*, in press.
(13) R. J. Gillespie and G. J. Schrobilgen, *Inorg. Chem.*, **13**, 1230 (1974).
(14) F. O. Sladky, P. A. Bulliner, N. Bartlett, B. G. DeBoer, and A. Zalkin, *Chem. Commun.*, 1048 (1968).
(15) N. Bartlett and D. H. Lohmann, *Proc. Chem. Soc., London*, 115 (1962).
(16) N. Bartlett, *Proc. Chem. Soc., London*, 218 (1962).
(17) N. Bartlett, S. P. Beaton, and N. K. Jha, *Chem. Commun.*, 168 (1966).
(18) J. Shamir, J. Binenboym, and H. H. Claassen, *J. Am. Chem., Soc.*, **90**, 6223 (1968).
(19) R. J. Gillespie and G. J. Schrobilgen, *Inorg. Chem.*, **13**, 765 (1974).
(20) R. J. Gillespie, B. Landa, and G. J. Schrobilgen, *Chem. Commun.*, 1543 (1971).
(21) R. J. Gillespie, B. Landa, and G. J. Schrobilgen, *J. Chem. Soc., Chem. Commun.*, 607 (1972).
(22) V. N. Prusakoa and V. B. Sokolov, *Russ. J. Phys. Chem. (Engl. Transl.)*, **45**, 1673 (1971).
(23) B. Lui and H. F. Schaefer, *J. Chem. Phys.*, **55**, 2369 (1971).
(24) N. Bartlett, M. Gennis, D. D. Gibler, B. K. Morrell, and A. Zalkin, *Inorg. Chem.*, **12**, 1717 (1973).
(25) A. M. Qureshi and F. Aubke, *Can. J. Chem.*, **48**, 3117 (1970).
(26) H. H. Claassen, G. L. Goodman, J. H. Holloway, and H. Selig, *J. Chem. Phys.*, **53**, 341 (1970).
(27) D. E. McKee, A. Zalkin, and N. Bartlett, *Inorg. Chem.*, **12**, 1713 (1973).
(28) We cannot provide any explanation for the absence of the strong 555-cm^{-1} band in the spectrum of a $Kr_2F_3^+SbF_6^-$ preparation reported by Holloway and Frlec.[9,11] Although these workers could possibly have isolated a low-temperature phase of $Kr_2F_3^+SbF_6^-$ containing a symmetric $Kr_2F_3^+$ cation, we have detected no sign of a phase change in our $Kr_2F_3^+SbF_6^-$ preparation at −80° after 1 week and at −196° after 3 days. In addition, we note that the $Kr_2F_3^+SbF_6^-$ samples prepared by these authors appear to be contaminated with $Kr_2F_3^+ \cdot xKrF_2 \cdot SbF_6^-$, and the lines which they ascribe to $KrF_2 \cdot KrF^+SbF_6^-$ can be readily assigned to $Kr_2F_3^+ \cdot xKrF_2 \cdot SbF_6^-$.
(29) J. Barr, R. J. Gillespie, and R. C. Thompson, *Inorg. Chem.*, **3**, 1149 (1964).
(30) J. Shamir and A. Netzer, *J. Sci. Instrum.*, **1**, 770 (1968).
(31) P. A. W. Dean and R. J. Gillespie, *J. Am. Chem. Soc.*, **91**, 7260 (1969).